Dynamical Approach to Multi-Equilibria Problems Considering the Debye–Hückel Theory of Electrolyte Solutions: Concentration Quotients as a Function of Ionic Strength

Ethan Zars, Joseph Schell, Marco A. Delarosa, Carmen Chicone & Rainer Glaser

Journal of Solution Chemistry

ISSN 0095-9782

J Solution Chem
DOI 10.1007/s10953-017-0593-z

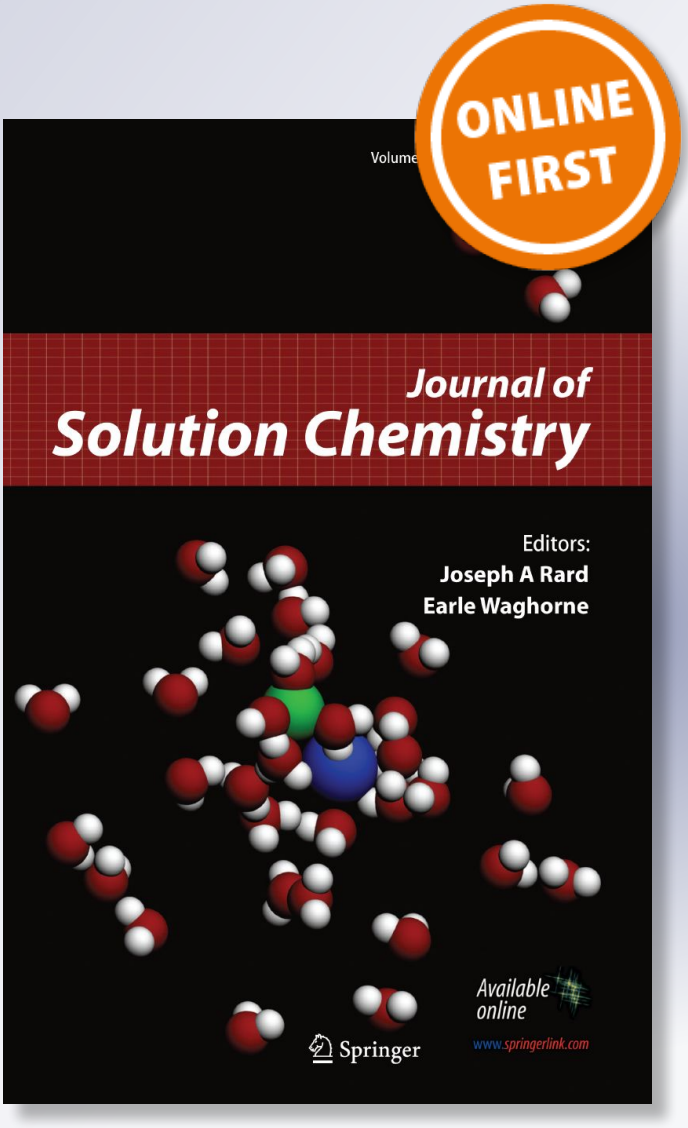

Springer

J Solution Chem
DOI 10.1007/s10953-017-0593-z

Dynamical Approach to Multi-Equilibria Problems Considering the Debye–Hückel Theory of Electrolyte Solutions: Concentration Quotients as a Function of Ionic Strength

Ethan Zars[1] · Joseph Schell[1] · Marco A. Delarosa[1,2] · Carmen Chicone[2] · Rainer Glaser[1]

Received: 31 October 2016 / Accepted: 22 December 2016

Abstract We recently described a dynamical approach to the equilibrium problem that involves the formulation of the kinetic rate equations for each species. The equilibrium concentrations are determined by evolving the initial concentrations via this dynamical system to their steady state values. This dynamical approach is particularly attractive because it can be extended easily to very large multi-equilibria systems and the effects of ionic strength also are easily included. Here we describe mathematical methods for the determination of steady state concentrations of all species with the consideration of their activities using several approximations of Debye–Hückel theory of electrolyte solutions. We describe the equations for a system that consists of a triprotic acid H_3A and its conjugate bases. With these equations, two types of multi-equilibria systems were studied and compared to experimental data. The first system is exemplified by case studies of solutions of acetate-buffered acetic acid and the second system is exemplified by the hydroxide titration of citric acid. The discussion focuses on the effect of ionic strength on pH and on the amplification of acidity by ionic strength. Ionic strength effects are shown to cause significant deviations from the widely used Henderson–Hasselbalch equation.

Keywords Equilibrium · Ordinary differential equations · Dynamical approach · Acids/bases · Ionic strength · Activity coefficient

Electronic supplementary material The online version of this article (doi:10.1007/s10953-017-0593-z) contains supplementary material, which is available to authorized users.

✉ Rainer Glaser
glaserr@missouri.edu

Carmen Chicone
chiconec@missouri.edu

[1] Department of Chemistry, University of Missouri, Columbia, MO 65211, USA

[2] Department of Mathematics, University of Missouri, Columbia, MO 65211, USA

Published online: 17 March 2017

1 Introduction

It is a fundamental problem in chemistry to calculate the pH of a buffer solution of known constituents and initial conditions. It is a related and important problem to calculate the concentration of each species at equilibrium corresponding to a pH value and initial conditions. Ionic strength affects these equilibrium concentrations [1, 2]. While species concentrations can be determined spectroscopically, it is the activity, however, which determines the kinetic behavior of a species and, hence, the multi-equilibria composition. The activity $a(S)$ of a species S is related to its concentration $[S]$ via the activity coefficients $f_z(I)$ which depend on the absolute value of the charge z of species S and on the ionic strength I of the solution, $a(S) = f_z\,(I)\cdot[S]$ (vide infra). Even though the solution chemistry community is well aware of the concept of ionic strength effects, nevertheless, it is commonly assumed that $a(S) \approx [S]$ to simplify the numerical solution of an equilibrium system and with the implied suggestion that activity coefficients f are not that different from unity. It is now possible to solve multi-equilibria with the proper consideration of activities, the usual assumptions can be tested, and it is found that the assumption may not hold, not even approximately, for electrolyte solutions that contain multiply charged species even at modest ionic strength [3–6]. In particular, we will show that activities do not only affect the argument of the logarithm in the widely used Henderson–Hasselbalch equation [7] but also alters the slope ($s \neq 1$) and the intercept ($r \neq 1$) significantly:

$$\mathrm{pH} = r\,\mathrm{pK_a} + s\log_{10}\frac{a(\mathrm{Ac^-})}{a(\mathrm{HAc})}$$

Citric acid and its conjugate bases (including the di- and trianions) are important in many chemical systems, ionic strength effects of citric acid systems have been studied and illustrate the point in a compelling fashion. Citric acid is known as an important metabolic intermediate in the ATP-producing citric acid cycle [8] which occurs inside the mitochondrial matrix at pH = 7.7 [9]. The ionic strength of the mitochondrial matrix can be up to 0.2 mol·L^{-1} and has been shown to have a strong impact on the electron transport chain [10]. The complexation constants of sodium ions with the various conjugate anions of citric acid (dihydrogen citrate, monohydrogen citrate) have been experimentally determined at various ionic strengths [11]. Citric acid is also part of a commonly used buffer system [12–15]. Citric acid can participate in reactions and some examples include the synthesis of pyrroles with citric acid catalysis [16], the important Pechini sol–gel method of synthesizing lithium–niobium powders using citrate as reducing agent [17–19], and the synthesis of gold nanoparticles by reduction of auric acid with citrate [20]. A citrate-rich environment has been found to speed up enzyme kinetics compared to a crowded, polymer rich environment [21]. Addition of calcium citrate into cells decreases the concentrations of reactive oxygen species in part because citrate itself has antioxidant properties [22] but also because citrate increases the activity of antioxidant enzymes, decreases nitric oxide concentration, and impacts gene expression [23]. Citrate has also been shown to inhibit cisplatin binding to DNA over a wide pH range [24].

We have recently compared the traditional equilibrium approach to the alternative dynamical approach as a way to calculate species concentrations at equilibrium [25]. The traditional equilibrium approach uses the definitions of the equilibrium constants ($1 + \sum_m n_m$ equations) together with conservation of mass (m equations) and conservation of charge (1 equation) to determine the concentrations of the ($2 + \sum_m n_m + m$) species. For multi-equilibria systems there is no explicit solution to this system of equations and,

thus, numerical methods must be employed. Usually, the $(2 + \sum_m n_m + m)$ equations are reduced to a single high-degree polynomial of one species (e.g., $[H^+]$). The chemically meaningful root of the polynomial is approximated and the concentrations of the other species are computed subsequently. The alternative dynamical approach is based on the kinetic rate equations for each species and this approach is commonly employed in biochemical analysis [26]. General mass action kinetics theory [27–29] allows one to formulate a system of ordinary differential equations (ODEs) for the time-dependent concentrations of the species involved in the reactions. We have shown how the steady-state solutions can be determined by solving this system of differential equations upon specification of the reaction rate constants and the initial concentrations [25].

While the conceptual framework for this dynamical approach is somewhat more sophisticated than the equilibrium approach, it has several advantages: there are well-established numerical methods available for the computation of all species as functions of time and the dynamical method scales easily with the addition of more types of acids. Moreover, the effects of ionic strength are easily included in the dynamical approach and it is the purpose of the current paper to describe the dynamical approach with consideration of several approximate extensions of the Debye–Hückel theory of electrolyte solutions. Specifically, we consider here the general case of the coupled equilibria given by Eqs. 1–4. Perhaps most importantly, the dynamical method lays the foundation for approaching dynamical problems in chemistry including oscillating reactions, pattern formations in reaction–diffusion systems, and many other processes in all areas of science and engineering [30–35].

$$H_2O \rightleftharpoons H^+ + OH^- \qquad K_w = [H^+][OH^-] \tag{1}$$

$$H_3A \rightleftharpoons H^+ + H_2A^- \qquad K_{11} = [H^+][H_2A^-]/[H_3A] \tag{2}$$

$$H_2A^- \rightleftharpoons H^+ + HA^{2-} \qquad K_{12} = [H^+][HA^{2-}]/[H_2A^-] \tag{3}$$

$$HA^{2-} \rightleftharpoons H^+ + A^{3-} \qquad K_{13} = [H^+][A^{3-}]/[HA^{2-}] \tag{4}$$

$$HA \rightleftharpoons H^+ + A^- \qquad K_{11} = [H^+][A^-]/[HA] \tag{5}$$

Equations 1–4 describe mixtures of a triprotic acid H_3A (acid 1) and its salts MH_2A, M_2HA and M_3A, where M represents an arbitrary singly-charged, inert, non-aggregated metal cation and the corresponding dissociation constants are K_w, K_{11}, K_{12}, and K_{13}. The equilibrium constant K_w is the ionic product of water, the acidity constants K_{mn} describe the equilibria for the nth dissociation of n-protic acid m. The dynamical approach to the system of Eqs. 1–4 allows for the study of buffered acids H_3A, H_2A and HA and their titrations with MOH. A simple buffered system is exemplified by the acetic acid–acetate buffer (example 1, Eqs. 1 and 2′) and a titration is exemplified by the hydroxide titration of citric acid (example 2). We studied these two simple systems to compare and confirm the dynamical method against experimental data [36]. We also compare our results to the few previously reported data computed with the equilibrium approach [37]. The discussion focuses on the effect of ionic strength on pH and on the amplification of acidity by ionic strength as well as the difference between the activities and concentrations of the intermediate deprotonation species.

2 Mathematical Methods

2.1 Dynamical Approach to Multi-Equilibria

General mass action kinetics theory [27–29] leads to the system of ordinary differential Eqs. 5–10 for the time-dependent concentrations of the species in reactions 1–4. We recently described the formulations of the differential equations for an H_2A/HB system [25] so we can be brief here.

$$\frac{d[H^+]}{dt} = k_{wf} - k_{wb}[H^+][OH^-] + k_{11f}[H_3A] - k_{11b}[H^+][H_2A^-] + k_{12f}[H_2A^-] - k_{12b}[H^+]\left[HA^{2-}\right] + k_{13f}\left[HA^{2-}\right] - k_{13b}[H^+]\left[A^{3-}\right] \tag{5}$$

$$\frac{d[OH^-]}{dt} = k_{wf} - k_{wb}[H^+][OH^-] \tag{6}$$

$$\frac{d[H_3A]}{dt} = -k_{11f}[H_3A] + k_{11b}[H^+][H_2A^-] \tag{7}$$

$$\frac{d[H_2A^-]}{dt} = k_{11f}[H_3A] - k_{11b}[H^+][H_2A^-] - k_{12f}[H_2A^-] + k_{12b}[H^+]\left[HA^{2-}\right] \tag{8}$$

$$\frac{d\left[HA^{2-}\right]}{dt} = k_{12f}[H_2A^-] - k_{12b}[H^+]\left[HA^{2-}\right] - k_{13f}\left[HA^{2-}\right] + k_{13b}[H^+]\left[A^{3-}\right] \tag{9}$$

$$\frac{d\left[A^{3-}\right]}{dt} = k_{13f}\left[HA^{2-}\right] - k_{13b}[H^+]\left[A^{3-}\right] \tag{10}$$

$$\frac{d[H^+]}{dt} = k_{wf} - k_{wb}[H^+][OH^-] + k_{11f}[HA] - k_{11b}[H^+][A^-] \tag{5'}$$

$$\frac{d[HA]}{dt} = -k_{11f}[HA] + k_{11b}[H^+][A^-] \tag{7'}$$

Every equilibrium reaction is described by two reaction rate constants; rate constant k_f for the forward reaction and rate constant k_b for the backward (reverse) reaction. These reaction rate constants are related via the equilibrium constant K by $K = k_f/k_b$. We refer to the reaction rate constants of reactions 1–4 using the subscript of the respective equilibrium constant and appending either "f" or "b" for forward or backward. Hence, the reaction rate constants k_{wf} and k_{wb} describe the autoionization of water (Eq. 1). We refer to the reaction rate constants for the forward and backward reactions of the first dissociation of H_3A (acid 1, Eq. 2) as k_{11f} and k_{11b}, respectively, and to the reaction rate constants for the forward and backward reactions of the dissociation of H_2A^-(Eq. 3) as k_{12f} and k_{12b}, respectively, and k_{13f} and k_{13b} are the reaction rate constants for the forward and backward reactions, respectively, of the dissociation of HA^{2-} (Eq. 4).

In the present context, we are interested in the determination of the concentrations of all species in aqueous solution *at equilibrium* at 298.15 K, and not in the transient kinetics of *reaching* the equilibrium. Hence, once the equilibrium constants are specified, we can freely choose in each case either the forward or backward reaction rate constant and then use the equation $K = k_f/k_b$ to determine the other. For all numerical computations in this paper, we used $k_{wf} = 10^{-3}$, $K_w = 10^{-14}$, $k_{11f} = 10^2$, $k_{12f} = 10^2$, $k_{13f} = 10^2$, and

$k_{2f} = 10^2$. In addition, all runs in example 1 used the initial concentrations $[H^+] = [OH^-] = 10^{-7}$ for the dissociation of water. For example 2, we used the same initial proton concentration and varied $[OH^-] = [OH^-]_0$. The remaining initial settings are specified below.

2.2 Dynamical Approach to Multi-Equilibria Accounting for Ionic Strength

The concentration quotients of Eqs. 1–4 describe the equilibrium constants for highly dilute solutions in which the overall ion concentration is negligible. In more concentrated solutions Eqs. 1–4 need to be replaced by the thermodynamic equilibrium constants in which all concentrations $[S]$ are replaced by activities $a\,(S)$ and one obtains Eqs. 11–14 [38]:

$$K_w^\theta = a(H^+)a(OH^-) = f_1^2 K_w^I \tag{11}$$

$$K_{11}^\theta = a(H^+)a(H_2A^-)/a(H_3A) = f_1^2 K_{11}^I \tag{12}$$

$$K_{12}^\theta = a(H^+)a\left(HA^{2-}\right)/a(H_2A^-) = f_2 K_{12}^I \tag{13}$$

$$K_{13}^\theta = a(H^+)a\left(A^{3-}\right)/a\left(HA^{2-}\right) = f_1 f_3/f_2 K_{13}^I \tag{14}$$

$$K_{11}^\theta = a(H^+)a(A^-)/a(HA) = f_1^2 K_{11}^I \tag{15}$$

In the Debye–Hückel theory of electrolyte solutions the activities $a(S)$ are related to the concentrations $[S]$ via the activity coefficients $f_z(I)$ that depend on the absolute value of the charge z of species S and on the ionic strength I. The concentration quotient of the nth dissociation of acid m as a function of ionic strength will be denoted as K_{mn}^I and the value will become equal to the equilibrium constant K_{mn} as the ionic strength approaches zero (Eq. 15). Ionic strength is defined by Eq. 16 and takes the form of Eqs. 17 or 17′ for the present cases.

$$K_{mn} = \lim_{I \to 0} K_{mn}^I \tag{15}$$

$$I = 0.5 \sum_i z_i^2 c(S_i) \tag{16}$$

$$I = 0.5\left([H^+] + [OH^-] + [H_2A^-] + 4\left[HA^{2-}\right] + 9\left[A^{3-}\right] + [OH^-]_0\right) \tag{17}$$

$$I = 0.5\left([H^+] + [OH^-] + [A^-] + [A^-]_0\right) \tag{17'}$$

The term $[OH^-]$ accounts for the cation of the hydroxide salt in example 2. The term $[A^-]_0$ accounts for the cation of the acetate salt in example 1. The relation between activity coefficient and ionic strength is provided by various forms of the Debye–Hückel equation [39, 40] including the Debye–Hückel limiting law (DHLL, Eq. 18.1), the extended Debye–Hückel equation (EDHE, Eq. 18.2), the Güntelberg variant [41] of EDHE (Eq. 18.3), and by Davies's extension [42] (Eq. 18.4) of Güntelberg's equation ($b = 0$).

$$\log_{10}(f_z) = -Az^2\sqrt{I} \quad \text{DHLL, if } I < 10^{-2.3} \text{ mol·L}^{-1} \tag{18.1}$$

$$\log_{10}(f_z) = -Az^2\frac{\sqrt{I}}{1+Ba\sqrt{I}} \quad \text{EDHE, if } I < 10^{-2.3} \text{ mol·L}^{-1} \tag{18.2}$$

$$\log_{10}(f_z) = -Az^2\frac{\sqrt{I}}{1+\sqrt{I}} \quad \text{Güntelberg, if } I < 0.1 \text{ mol·L}^{-1} \tag{18.3}$$

$$\log_{10}(f_z) = -Az^2\left(\frac{\sqrt{I}}{1+\sqrt{I}} - bI\right) \quad \text{Davies, if } I < 0.5 \text{ mol·L}^{-1} \tag{18.4}$$

The parameters A and B are the Debye–Hückel coefficients $A = e^2B/(2.3038\pi\varepsilon_0\varepsilon_r kT)$ and $B = \left\{\frac{2e^2N_L}{\varepsilon_0\varepsilon_r kT}\right\}^{0.5}$ (Avogadro's number N_L, electronic charge e, static dielectric constant (relative permittivity) of water ε, Boltzmann's constant k, temperature T) and a is an adjustable parameter depending on the size of the ion (in Å). For water at room temperature $A \approx 0.5085$ and $B \approx 0.3281 \times 10^{-8}$ [39] and we employed $A = 0.51$ [40]. The parameter b in the Davies equation was set to $b = 0.2$ L·mol^{-1} [42] and, in a few cases, we will also employ $b = 0.1$ L·mol^{-1} for reasons given below. The Davies equation is believed to give a possible error of 3% at $I = 0.1$ mol·L^{-1} and 10% at $I = 0.5$ mol·L^{-1} [40].

With the activity coefficient f_1(t) and $f_2(t)$ for singly and doubly charged species, respectively, the ODEs of Eqs. 5–10 become:

$$\frac{d[\mathrm{H^+}]}{dt} = k_{\mathrm{wf}} - k_{\mathrm{wb}}f_1^2[\mathrm{H^+}][\mathrm{OH^-}] + k_{11\mathrm{f}}[\mathrm{H_3A}] - k_{11\mathrm{b}}f_1^2[\mathrm{H^+}][\mathrm{H_2A^-}] + k_{12\mathrm{f}}f_1[\mathrm{H_2A^-}] - k_{12\mathrm{b}}f_1f_2[\mathrm{H^+}]\left[\mathrm{HA^{2-}}\right] + k_{13\mathrm{f}}f_2\left[\mathrm{HA^{2-}}\right] - k_{13\mathrm{b}}f_1f_3[\mathrm{H^+}]\left[\mathrm{A^{3-}}\right] \tag{19}$$

$$\frac{d[\mathrm{OH^-}]}{dt} = k_{\mathrm{wf}} - k_{\mathrm{wb}}f_1^2[\mathrm{H^+}][\mathrm{OH^-}] \tag{20}$$

$$\frac{d[\mathrm{H_3A}]}{dt} = -k_{11\mathrm{f}}[\mathrm{H_3A}] + k_{11\mathrm{b}}f_1^2[\mathrm{H^+}][\mathrm{H_2A^-}] \tag{21}$$

$$\frac{d[\mathrm{H_2A^-}]}{dt} = k_{11\mathrm{f}}[\mathrm{H_3A}] - k_{11\mathrm{b}}f_1^2[\mathrm{H^+}][\mathrm{H_2A^-}] - k_{12\mathrm{f}}f_1[\mathrm{H_2A^-}] + k_{12\mathrm{b}}f_1f_2[\mathrm{H^+}]\left[\mathrm{HA^{2-}}\right] \tag{22}$$

$$\frac{d\left[\mathrm{HA^{2-}}\right]}{dt} = k_{12\mathrm{f}}f_1[\mathrm{H_2A^-}] - k_{12\mathrm{b}}f_1f_2[\mathrm{H^+}]\left[\mathrm{HA^{2-}}\right] - k_{13\mathrm{f}}f_2\left[\mathrm{HA^{2-}}\right] + k_{13\mathrm{b}}f_1f_3[\mathrm{H^+}]\left[\mathrm{A^{3-}}\right] \tag{23}$$

$$\frac{d\left[\mathrm{A^{3-}}\right]}{dt} = k_{13\mathrm{f}}f_2\left[\mathrm{HA^{2-}}\right] - k_{13\mathrm{b}}f_1f_3[\mathrm{H^+}]\left[\mathrm{A^{3-}}\right] \tag{24}$$

$$\frac{d[\mathrm{H^+}]}{dt} = k_{\mathrm{wf}} - k_{\mathrm{wb}}f_1^2[\mathrm{H^+}][\mathrm{OH^-}] + k_{11\mathrm{f}}[\mathrm{HA}] - k_{11\mathrm{b}}f_1^2[\mathrm{H^+}][\mathrm{A^-}] \tag{25}$$

$$\frac{d[\mathrm{HA}]}{dt} = -k_{11\mathrm{f}}[\mathrm{HA}] + k_{11\mathrm{b}}f_1^2[\mathrm{H^+}][\mathrm{A^-}] \tag{26}$$

The numerical solution of Eqs. 19–24 (19′, 20, 21′) determines the concentrations of all species *at equilibrium*, because they satisfy the equilibrium expressions of Eqs. 11–14 (11 and 12′) which account for the effects of ionic strength at equilibrium.

2.3 Numerical Determination of Steady State Concentrations

An effective method to determine the steady state concentrations for a given set of initial concentrations simply involves the use of a numerical method [43] to approximate the solutions of the differential equations forward in time until the computed concentrations remain unchanged up to some pre-specified accuracy over some pre-specified time interval. We approximated solutions of the system of differential equations using the *Mathematica* [44, 45] solver NDSolve [46]. It is not possible to conclude with absolute certainty that an equilibrium was indeed reached at the end of the integration of the dynamic equations. However, we showed previously [25] that, for the dynamic Eqs. 5–10 (5′, 6 and 7′) describing the equilibria of reactions 1–4 (1 and 2′), that the equilibrium approach and the dynamic approach produce that same result. Importantly, we can be confident in the computed values because of their excellent agreement with the measured data.

3 Results and Discussion

3.1 Example 1: Acetate-Buffered Acetic Acid

We studied simple acetate buffered acetic acid systems to compare our results (Table 1) to published experimental data [36]. In addition, we computed results for a series of solutions with $[HAc]_0 = 0.051$ mol·L^{-1} and evaluated the system of dynamical Eqs. 5′, 6 and 7′ with 19′, 20–21′ for each new initial concentration of acetate salt ranging from pure acetic acid to aqueous acetic acid containing up to 0.104 mol·L^{-1} of added acetate, i.e., twice the concentration of acetic acid. The results of these calculations are shown in Figs. 1 and 2.

Table 1 shows the data computed with the Davies method with $b = 0.1$ L·mol^{-1}. A more extensive Table S1 is provided as part of Supplementary Material and also lists data computed with the values $b = 0$ and $b = 0.2$ L·mol^{-1}. The value $b = 0.1$ L·mol^{-1} was used by Perrin and Dempsey [36] (p. 7, Eq. 2.11) with reference to an early paper by Davies [47] and also was employed in Ref. [37]. However, we note that Davies consistently employed $b = 0.2$ L·mol^{-1} in his papers [42, 47]. The data (in Table S1) show that the pH values computed with any one of the Debye–Hückel methods give just about the same results (differences below 0.1).

Table 1 contains the values $pH_{con} = -\log_{10}([H^+])$ computed based on the proton concentrations and the values $pH_{act} = -\log_{10}\{a(H^+)\}$ computed with the proton activities. Experimental methods of pH determination rely on indicator equilibria or electrode equilibria and thus measure proton activity. Consequently, the experimental data reported in Table 1 need to be compared to computed pH_{act} values. The pH_{act} values computed with the DH methods are generally in better agreement with the experimental measurements (average absolute deviation of 0.032 ± 0.030) than the data computed without consideration of ionic strength (average absolute deviation of 0.180 ± 0.046).

Figure 1 shows plots of the pH_{act} of the solution as a function of the initial acetate concentration and as a function of $\log_{10}\{a(Ac^-)/[HAc]\}$ to illustrate a Henderson–

Table 1 Comparison of experimental and computed pH values

Multi-equlibria system		Ref. [36][a]	Our calculations			Ref. [37] method	
HAc ($mol \cdot L^{-1}$)	NaAc ($mol \cdot L^{-1}$)	pH_{exp}	pH_{con} $I = 0$	pH_{con} $b = 0.1$ Davies	pH_{act} $b = 0.1$ Davies	pH_{con} $b = 0.1$ Davies	pH_{act} $b = 0.1$ Davies
0.0926	0.0074	3.6	3.68	3.60	3.63	3.60	3.64
0.088	0.012	3.8	3.90	3.80	3.84	3.80	3.85
0.082	0.018	4.0	4.10	3.99	4.03	3.99	4.04
0.0736	0.0264	4.2	4.32	4.18	4.23	4.18	4.25
0.061	0.039	4.4	4.57	4.40	4.46	4.40	4.48
0.051	0.049	4.6	4.74[d]	4.56	4.63	4.56	4.65[c]
0.04	0.06	4.8	4.94	4.74	4.82	4.74	4.84
0.0296	0.0704	5.0	5.14	4.93	5.01	4.93	5.03
0.021	0.079	5.2	5.34	5.12	5.20	5.12	5.23
0.0176	0.0824	5.4	5.43	5.21	5.30	5.21	5.32
0.0096	0.0904	5.6	5.73	5.51	5.59	5.51	5.62
Citric acid ($mol \cdot L^{-1}$)	NaOH ($mol \cdot L^{-1}$)						
0.2	0.02	2.15	2.29	2.19	2.26	2.17	2.24
0.2	0.04	2.39	2.56	2.43	2.52	2.40	2.48
0.2	0.06	2.58	2.77	2.62	2.72	2.57	2.67
0.2	0.08	2.75	2.95	2.77	2.88	2.72	2.83
0.2	0.10	2.89	3.11	2.91	3.03	2.86	2.98
0.2	0.12	3.04	3.26	3.04	3.17	2.98	3.11
0.2	0.14	3.18	3.42[d]	3.17	3.31	3.11	3.24[c]
0.2	0.16	3.32	3.59	3.30	3.44	3.23	3.38
0.2	0.18	3.46	3.76	3.43	3.58	3.36	3.51
0.2	0.20	3.59	3.94	3.56	3.71	3.48	3.64
0.2	0.22	3.75	4.13	3.68	3.84	3.60	3.76

Table 1 continued

Citric acid ($mol \cdot L^{-1}$)	NaOH ($mol \cdot L^{-1}$)						
0.2	0.24	3.90	4.30	3.80	3.96	3.72	3.88
0.2	0.26	4.03	4.46	3.91	4.08	3.83	4.00
0.2	0.28	4.14	4.61	4.02	4.19	3.94	4.12
0.2	0.30	4.27	4.76	4.13	4.30	4.05	4.23
0.2	0.32	4.37	4.91	4.23	4.41	4.16	4.34
0.2	0.34	4.50	5.06[d]	4.34	4.53	4.27	4.45[c]
0.2	0.36	4.62	5.22	4.45	4.64	4.38	4.57
0.2	0.38	4.74	5.40	4.57	4.76	4.50	4.69
0.2	0.40	4.87	5.58	4.68	4.88	4.62	4.81
0.2	0.42[b]	4.98	5.77	4.80	5.00	4.74	4.94
0.2	0.44	5.11	5.94	4.92	5.12	4.86	5.06
0.2	0.46	5.21	6.11	5.04	5.24	4.99	5.19
0.2	0.48[b]	5.34	6.27	5.16	5.36	5.11	5.32
0.2	0.50	5.49	6.43	5.29	5.49	5.25	5.45
0.2	0.52	5.63	6.59	5.43	5.64	5.40	5.60
0.2	0.54[b]	5.80	6.78	5.60	5.81	5.57	5.77
0.2	0.56[b]	6.02	7.01[d]	5.82	6.02	5.79	5.99[c]
0.2	0.58[b]	6.33	7.36	6.15	6.36	6.13	6.34
0.2	0.59[b]	6.51	7.68	6.47	6.67	6.45	6.66

[a] Experimental data for citric acid titration reported to two digits, see Table 10.9 in Ref. [36]. Experimental data for acetic acid buffer reported to one digit, see Table 10.18 in Ref. [36]. Units of b, $L \cdot mol^{-1}$

[b] Ionic strength values are given in Fig. 5. The I values allow the determination of the highest pH values for which the above data and the graphs in Fig. 3 are within the recommended limits of the respective approximations

[c] Values computed with the Baeza–Baeza method and matching data in Ref. [37]

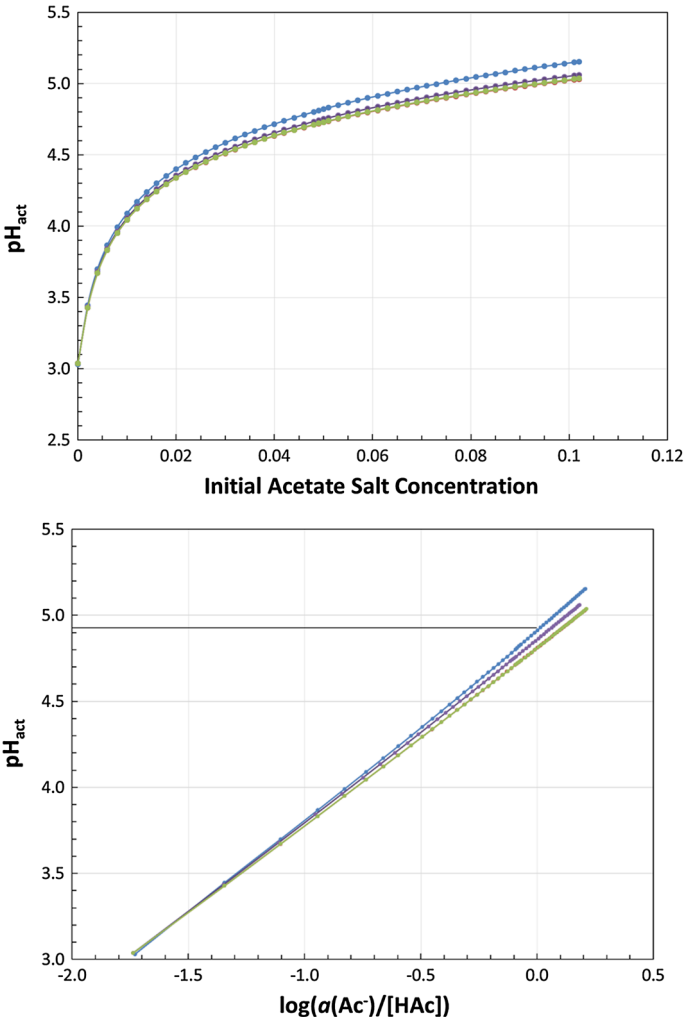

Fig. 1 Computed pH_{act} values of acetate-buffered acetic acid. *Top* pH_{act} as a function of added acetate. *Bottom* pH_{act} as a function of $\log_{10}\{a(Ac^-)/[HAc]\} = -\log_{10}\{[HAc]/a(Ac^-)\}$. *Line color* represents approximations to the Debye–Hückel (DH) theory: $I = 0$ (*top curve* in both plots, *blue*, $pH_{act} = 4.9115 + 1.1067\ \log_{10}\{a(Ac^-)/[HAc])\}$, Davies equation with $b = 0.1$ L·mol^{-1} (*middle curve* in both plots, *purple*, $pH_{act} = 4.8591 + 1.0633\ \log_{10}\{a(Ac^-)/[HAc])\}$ or $b = 0.2$ L·mol^{-1} [*lowest curve* in both plots, *green*, $pH_{act} = 4.8106 + 1.0336\ \log_{10}\{a(Ac^-)/[HAc]\}$, overlaps with the Güntelberg curve, $pH_{act} = 4.8107 + 1.0336\ \log_{10}\{a(Ac^-)/[HAc]\}$] (Color figure online)

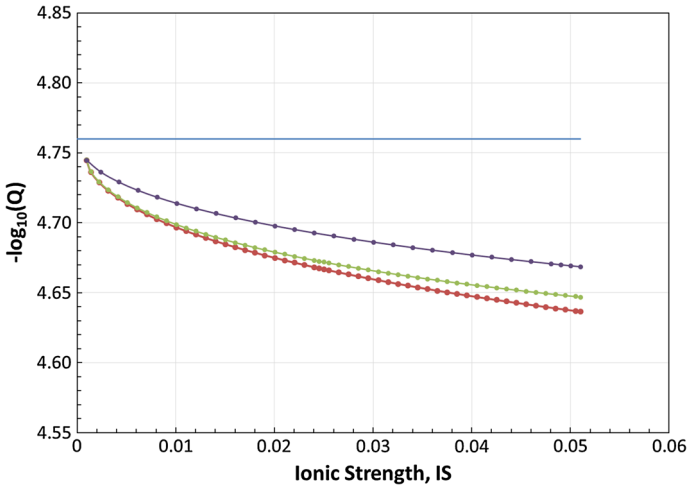

Fig. 2 Ionic strength effects on species concentration in acetate-buffered acetic acid. Negative logarithm of concentration quotient $\{-\log_{10}(Q)\}$ as a function of ionic strength with $Q = K_a^I = [H^+][Ac^-]/[HAc]$. *Line color* represents various approximations to the Debye–Hückel (DH) theory: $I = 0$ (*blue*, horizontal line for pK_a(HAc) and, from top to bottom, Davies with $b = 0.1$ L·mol^{-1} (*purple*) or $b = 0.2$ L·mol^{-1} (*green*), and Güntelberg (*red*) (Color figure online)

Hasselbalch type equation (Eq. 25a). Analogous plots for pH_{con} are shown in Fig. S1 in the Supplementary Material.

$$pH_{con} = pK_a + \log_{10}\frac{[Ac^-]}{[HAc]} \tag{25c}$$

$$pH_{act} = pK_a' + s\log_{10}\frac{a(Ac^-)}{a(HAc)} \tag{25a}$$

The plots show a linear relationship between pH_{act} and $\log_{10}\{a(Ac^-)/[HAc]\}$ which is expected. The curves calculated with ionic strength effects all lie below the curve calculated without ionic strength effects, which is also expected. Note, however, that the pH_{act} where $\log_{10}\{a(Ac^-)/[HAc]\} = 0$ is well above $pK_a = 4.76$ for all those curves (Eq. 25a); $pK_a' > pK_a$ and $s > 1$. With decreasing ionic strength, the curves coalesce and approach the Henderson–Hasselbalch equation (Eq. 25c). This condition is only seen in Fig. S1 where pH_{con} is plotted against $\log_{10}([Ac^-]/[HAc])$ for the case of no ionic strength effects.

The concentration quotient is defined as $K_a^I = [H^+][Ac^-]/[HAc] = Q$, and Fig. 2 shows the dependence of the negative logarithm of this concentration quotient on ionic strength. The horizontal line at the pK_a value of acetic acid serves as a reference; this is the limit of $-\log_{10}(K_a^I)$ as the value of I approaches zero. Figure 2 clearly shows that the concentration quotient increases with ionic strength, i.e., the $-\log_{10}(Q)$ curves all are below the blue reference line. The ionic strength curves in Fig. 2 do not extend all the way to $I = 0$ and they never reach $-\log_{10}(Q) = pK_{act}$ because acetic acid will dissociate to some degree in aqueous solution and create a non-zero I even in the absence of any added salt. Note that the order of the curves *does not* follow the size of the b value; the $b = 0.2$ L·mol^{-1} curve (green) lies between the $b = 0.1$ L·mol^{-1} curve (purple) and the $b = 0$ curve (red).

Effectively, an increase of the ionic strength makes an acid more acidic. This increase of the acidity can be easily understood considering the dynamic equations and the role of the activity coefficients. Within the I range in which the Davies equation is applicable, the activity coefficient f will always be less than one, its value will steadily decrease as the ionic strength increases (Eq. 18), and the decrease is steepest in the low I region. In the dynamical equation for proton concentration (Eq. 19′), the only terms without activity coefficients are forward rates which increase with proton concentration. In contrast, activity coefficients reduce the backward rates and slow the protonation of all conjugate bases.

3.2 Example 2: Hydroxide Titration of 0.2 Mol·L^{-1} Citric Acid

The titration of citric acid with hydroxide was studied to confirm the dynamical method against the experimental results of Perrin and Dempsey [36] and to examine activity effects for a triprotic acid. We employed the same pK_a values of 3.13, 4.76, and 6.40 for citric acid as in Ref. [37] and evaluated the multi-equilibria for the fixed concentration of citric acid at 0.2 mol·L^{-1} and various initial concentrations of hydroxide up to 0.59 mol·L^{-1}. The results are listed in the lower part of Table 1 and illustrated in Figs. 3, 4, 5. To help with the interpretation of the data, we also computed the respective results for a triprotic model acid with pK_a values of 3, 6, and 9, and these results are shown in Figs. S7, S8, and S9. The differences between the pK_a values of citric acid are about 1.6 $\{\Delta pK_a(1,2) = pK_{12} - - pK_{11} = 1.63; \Delta pK_a(2,3) = pK_{13} - pK_{12} = 1.64\}$ and the pK_{act} values of the triprotic model acid are further apart $\{\Delta pK_{act}(1,2) = \Delta pK_{act}(2,3) = 3\}$.

The data in Table 1 show that the consideration of ionic strength becomes imperative and that the choice among the various Debye–Hückel methods matters in this case. The average absolute deviations from the measured pH$_{act}$ values and their standard deviations

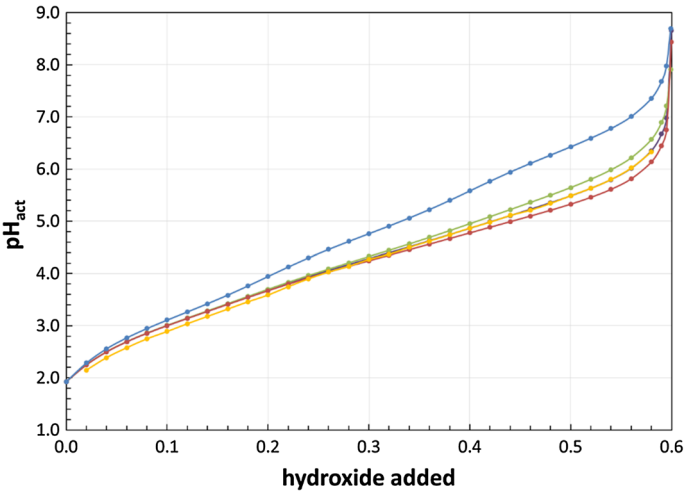

Fig. 3 Computed pH$_{act}$ values of hydroxide titration of 0.2 mol·L^{-1} citric acid as a function of added hydroxide. From top to bottom (at $[OH^-]_0 > 0.3$ mol·L^{-1}): $I = 0$ (*blue*), Davies with $b = 0.2$ L·mol^{-1} (*green*), experimental data (*orange*) overlay Davies curve with $b = 0.1$ L·mol^{-1} (*purple*) and Güntelberg ($b = 0$, *red*) (Color figure online)

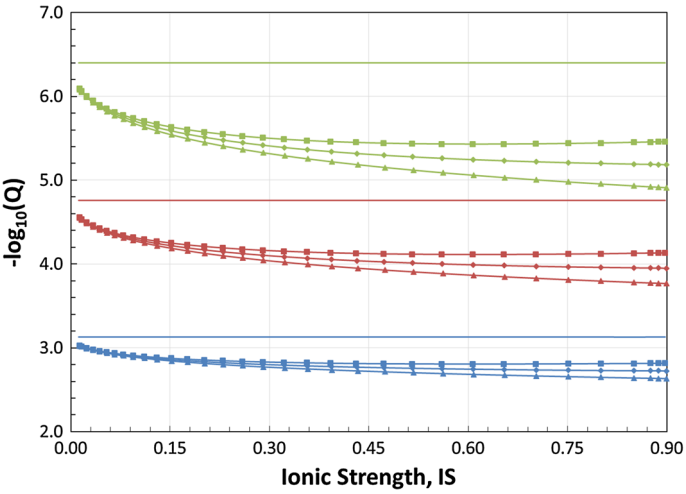

Fig. 4 Hydroxide titration of 0.2 mol·L^{-1} citric acid. Negative logarithm of concentration quotient $\{-\log_{10}(Q)\}$ as a function of ionic strength (I) with $Q = K_a^{\prime} = [H^+][B^-]/[HB]$. *Line color* represents acid dissociation number: first (*blue*, *bottom bundle*), second (*red*, *center bundle*), and third (*green*, *top bundle*). *Marker shape* represents DH method: $I = 0$ (*no marker*), Güntelberg (*triangle*), Davies with $b = 0.1$ L·mol^{-1} (*circle*) or $b = 0.2$ L·mol^{-1} (*square*) (Color figure online)

are: 0.56 ± 0.31 ($I = 0$), 0.09 ± 0.05 ($b = 0$), 0.05 ± 0.05 ($b = 0.1$ L·mol^{-1}), and 0.12 ± 0.07 ($b = 0.2$ L·mol^{-1}).

Figure 3 shows the pH_{act} of the solution at equilibrium as a function of $[OH^-]_0$. While all the curves start and end more or less at the same point, the curves for all of the DH approximations are considerably lower than the $I = 0$ curve. This is consistent with the titration curve in Fig. 1. As with Fig. 2, we find that the pH_{act} values decrease in the order pH (Davies, $b = 0.2$ L·mol^{-1}) > pH (Davies, $b = 0.1$ L·mol^{-1}) > pH (Güntelberg, $b = 0$) for a given value of added hydroxide. The divergence becomes significant around $[OH^-]_0 \approx 0.25$ mol·L^{-1} and it is especially large in the region $[OH^-]_0 \approx 0.54$ mol·L^{-1}. Note that the $b = 0.1$ L·mol^{-1} curve (purple) provides an almost perfect match of the experimental data (orange curve) for pH >4. In the region $[OH^-]_{added} \geq 0.26$ mol·L^{-1} the average absolute deviations from the measured pH_{act} values and their standard deviations are 0.10 ± 0.07 ($b = 0$), 0.02 ± 0.03 ($b = 0.1$ L·mol^{-1}), and 0.13 ± 0.08 ($b = 0.2$ L·mol^{-1}).

In Fig. 4 $-\log_{10}(Q)$ is shown as a function of I for the different DH approximations, much like Fig. 2 for the acetate buffer. The horizontal lines mark the pK_a values of citric acid and serve as a reference. Consistent with the findings from Fig. 2, the DH approximation curves are always lower than the pK_a and never reach the pK_a line. Ionic strength makes an acid more acidic and the example of citric acid illustrates that the increase in acidity is larger for the higher dissociations. At $I = 0.1$ mol·L^{-1}, for example, the Davies ($b = 0.2$ L·mol^{-1}) method shows that the value of $-\log_{10}(Q)$ is reduced by 0.22, 0.44, and 0.66, respectively, for the first, second, and third dissociation, respectively. These findings are consistent with another study that showed that increasing ionic strength itself leads to increased deprotonation of phthalic acid [48].

Figure 5 shows the concentrations of citric acid and of all of its deprotonated species as a function of pH. We first discuss the major effects of ionic strength by comparison of one

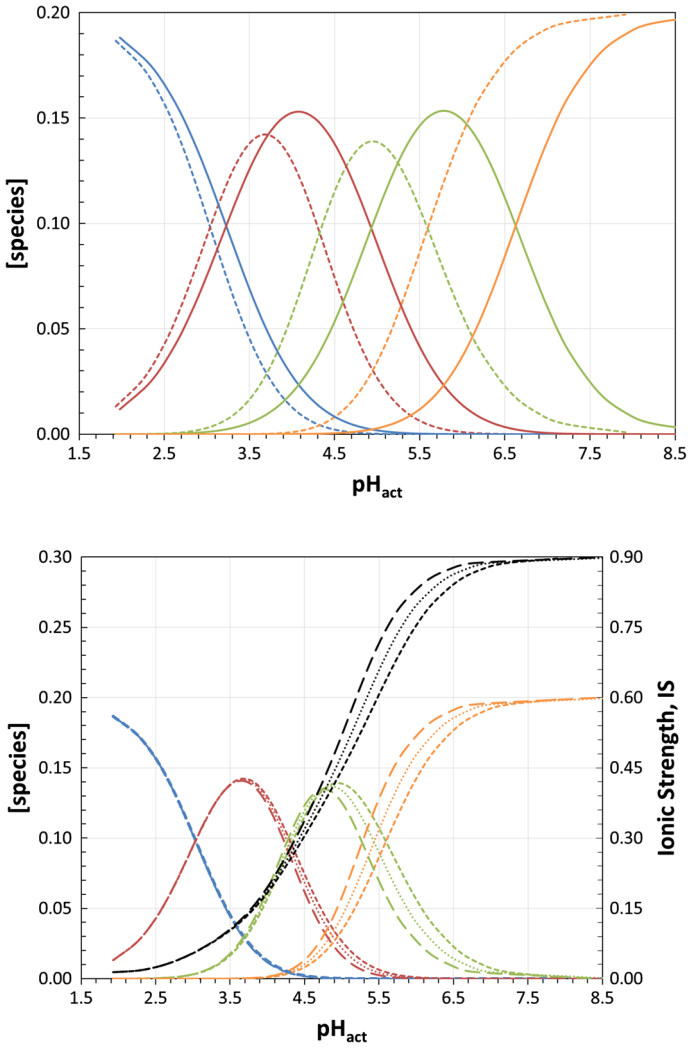

Fig. 5 Species concentrations in hydroxide titration of 0.2 mol·L^{-1} citric acid. With maxima occurring from left to right: concentration of H_3A (*blue*), H_2A^- (*red*), HA^{2-} (*green*) and A^{3-} (*orange*) as a function of pH_{act}. *Line* style indicates the Debye–Hückel approximation: $I = 0$ (*solid*), Güntelberg (*long dash*), Davies with $b = 0.1$ L·mol^{-1} (*dotted*) or $b = 0.2$ L·mol^{-1} (*short dash*). *Top* ionic strength effect on concentrations. *Bottom* effect of the DH approximations on concentrations. Curves terminating at $I = 0.9$ mol·L^{-1} (black) show ionic strength calculated from the three DH methods (Color figure online)

Davies curve to the $I = 0$ curve (top), and we then compare differences between the DH approaches (bottom).

The graph on top of Fig. 5 shows the curves computed with the Davies method with $b = 0.2$ L·mol^{-1} (dash) and for $I = 0$ curve (solid) for all relevant species. The Davies curves all are noticeably shifted to the left of the $I = 0$ curves, that is, the dissociations of all acids occur at a relatively lower pH when ionic strength is considered. This observation is consistent with the finding in example 1. It is one consequence that the maxima of the Davies curves for H_3A (blue), H_2A^- (red), and HA^{2-} (green) all are shifted to the left and

lower compared to the $I = 0$ curves. The Davies curve for $[A^{3-}]$ is always higher than the $I = 0$ curve. This is expected because the fully deprotonated species A^{3-} is the product of all previous acid dissociations and, since ionic strength makes acids more acidic, it should also increase the concentration of the conjugate base.

When the concentrations of species are graphed against pH_{act} instead of pH_{con} the peak concentrations are shifted to higher pH values (Fig. S5). These higher pH values reflect the pH values measured by standard industrial pH meters and is due to the fact that the activity of hydrogen ions is lower than its concentration.

The relative heights of the maxima of $[H_2A^-]$ and $[HA^{2-}]$ depend on the difference between the adjacent pK_a values. Large differences between the three pK_a values allows for high maxima and this is illustrated for the triprotic model acid in Fig. S4. In that case, there will be two major species present in every pH region, i.e., $H_{3-x}A^{x-}$ and $H_{2-x}A^{(x+1)-}$ ($x = 0, 1, 2$). In contrast, smaller ΔpK_a values diminish the maximum heights of the $[H_2A^-]$ and $[HA^{2-}]$ curves and each anion $H_{2-x}A^{(x+1)-}$ ($x = 0, 1$) will be accompanied by significant concentrations of both its conjugate acid and base.

We now consider the graph on the bottom of Fig. 4 and examine the differences between the three DH approximations. This graph also contains ionic strength curves for the three DH approximations as a function of pH using the secondary y-axis. We find that the curves are shifted to the left and this shift increases in the order Davies equation ($b = 0.2$ L·mol^{-1}) < Davies equation ($b = 0.1$ L·mol^{-1}) < Güntelberg equation ($b = 0$). All three approximation methods give almost the same concentration curves for citric acid. The concentration curves of dihydrogen citrate diverge markedly only on the high-pH side of their respective curves, whereas the concentration curves of monohydrogen citrate diverge even before the maximum is reached (i.e., at pH $\approx$ 3.7) and the divergence grows drastically with increasing pH. Finally, the $[A^{3-}]$ curves diverge almost immediately and stay apart until pH > 7. These results support the recommendation that the Güntelberg approximation is valid for $I < 0.1$ mol·L^{-1} (i.e., pH $\approx$ 3.3 in Fig. 4). Note that I reaches 0.5 mol·L^{-1} around pH $\approx$ 5.0 and the Davies approximation depends greatly on the b value as early as the trianion grows in.

The ionic strength curves show similar patterns of divergence and convergence. The ionic strength curves stay close together through the first dissociation of citric acid and they start to diverge in the region where $[H_2A^-] \approx [HA^{2-}]$ and $[A^{3-}]$ begins to grow in at $I \approx 0.2$ mol·L^{-1}. Maximal divergence occurs in the region where $[HA^{2-}] \approx [A^{3-}]$. Finally, in the pH $\geq$ 7 region, only the trianion remains in a significant concentration and the ionic strength curves converge. In the high pH regions the trianion is the dominant species in solution and its concentration approaches the initial citric acid concentration of 0.2 mol·L^{-1}. Since ionic strength itself is calculated in the same way, it is dependent only on the equilibrium concentrations that result from the different DH approximations. It is not surprising that the appearance of the trianion marks the beginning of the region of greatest divergence in the DH concentration curves. In the dynamical equations (cf. Eqs. 19–24) each species concentration is multiplied by an activity coefficient f_i which depends on ionic strength, and the ionic strength is highly sensitive to the trianion concentration (factor 9 in Eqs. 19, 23, and 24).

Figure 6 compares species concentrations and species activities of citric acid and its conjugate bases as a function of pH_{act} using the Davies equation $b = 0.1$ L·mol^{-1} method. Obviously, the concentration of citric acid is equal to its activity. It is also clear that the activities for all charged species are lower than their concentrations because activity coefficients always have to be less than one for this system. The difference between the concentration of a species and its activity increases with the degree of deprotonation from

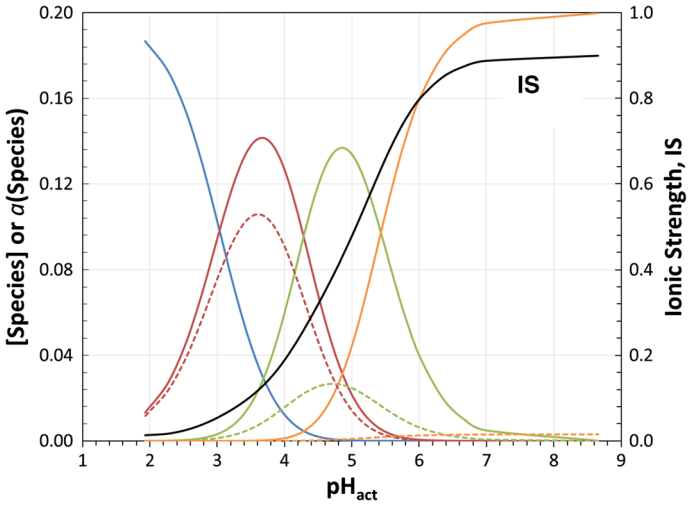

Fig. 6 Difference between species concentrations and species activities in hydroxide titration of 0.2 mol·L^{-1} citric acid. With maxima occurring from left to right: concentrations of H_3A (*solid blue*), H_2A^- (*solid red*), HA^{2-} (*solid green*) and A^{3-} (*solid orange*) and activities of H_2A^- (*dashed red*), HA^{2-} (*dashed green*) and A^{3-} (*dashed orange*), respectively, as a function of pH_{act}. All lines calculated using the Davies equation with $b = 0.1$ L·mol^{-1} approximation. The *solid black curve* shows ionic strength calculated from the Davies equation with $b = 0$ L·mol^{-1} using the secondary *y-axis* shown on the *right* side of the plot (Color figure online)

H_2A^- via HA^{2-} to A^{3-} and this is shown in Fig. 6. What we find to be remarkable about Fig. 6 is the fact that the ratio between activity and concentration can be *very small and nowhere near unity*. For example, the maximum HA^{2-} concentration occurs at $pH_{act} = 3.56$ and $f = 0.31$. For the A^{3-} species the ratio of activity to concentration is even smaller and, for example, at $pH_{act} = 6.51$ we find $f = 0.015$. The numerical data presented here show in a compelling fashion that the frequently made assumption of $c(S) \approx a(S)$ is clearly not warranted.

There are two reasons for the rather small activity coefficients in the higher pH range. First, the activity coefficient decreases with the square of the ion charge (Eq. 18). Second, and here is the important synergism, the activity coefficient decreases with ionic strength and the ionic strength itself (Eq. 16) is greatly increased in the higher pH range where the higher charged species are dominant in solution.

It is important to remember that the concentration of a species is what is detected by spectroscopic methods whereas the activity of the species is what determines the kinetic effect of the species. In the region of high pH and high ionic strength the *activities of all species are very low*, but the *concentration* of the trianion A^{3-} is quite large. Even the dianion HA^{2-} shows a low activity at its maximum concentration around pH = 5. The disparity between concentration and activity at higher pH values and ionic strengths means that the spectroscopic determination of a concentration would have very little bearing on the actual kinetic effect of the charged species.

4 Conclusions

The dynamical approach to the multi-equilibria problem involves the formulation of the kinetic rate equations for each species and the equilibrium concentrations are determined by evolving the initial concentrations via this dynamical system to their steady state. This dynamical approach is particularly attractive because it can be extended easily to very large multi-equilibria systems without the difficulty of reducing the equilibrium equations to a single high order polynomial and its numerical solution. There is another advantage of the dynamical approach that the effects of ionic strength also are easily included, and we have demonstrated this advantage with the present paper.

We described mathematical methods for the determination of steady state concentrations of all species with the consideration of their activities using several approximations of the Debye–Hückel theory of electrolyte solutions. The kinetic rate equations were provided for a multi-equilibria system consisting of a triprotic acid H_3A and its conjugate bases (Eqs. 1–4).

The dynamical approach to the system of Eqs. 1 and 2′ is exemplified by solutions of acetate-buffered acetic acid (example 1) and the system of Eqs. 1–4 is exemplified by the hydroxide titration of citric acid (example 2). These two examples were studied to compare the results of the dynamical method with available experimental data. Example 1 presents a low-I scenario and for this case the pH values computed with any one of the DH methods closely agree with each other and they are in better agreement with experiment than the data computed without consideration of ionic strength. On the other hand, example 2 presents high-I scenarios and the choice among the various Debye–Hückel methods matters in this case. The pH values computed with the Davies method and $b = 0.1\ \mathrm{L{\cdot}mol^{-1}}$ show the best agreement with experiment, and the match is especially remarkable in the $I \geq 0.25\ \mathrm{mol{\cdot}L^{-1}}$ region.

A common aspect of the discussion of both examples concerns the amplification of acidity by ionic strength. The computed concentration quotients demonstrate in a compelling fashion that an increase of ionic strength leads to an increase of the acidity of every acid. This increase of the acidity can be easily understood considering the dynamic equations and the role of the activity coefficients. It was also shown in Fig. 6 that, in higher pH ranges and higher ionic strengths, the activities of doubly and triply charged species are considerably lower than their concentrations and the assumption that activity is approximately equal to concentration cannot be made in these cases.

There is, however, deviation between our calculated pH values and the experimental values as can be seen in Fig. 3. The model for ionic strength that we used was a simple model that did not include some possible components of salt solutions. Specific interactions between species in solution could be occurring which would result in behavior not consistent with our treatment of ionic strength effects [38]. Ionic strength can also have effects on uncharged species that we did not consider in our model [49]. Even with these possible effects in salt solutions our calculated data agrees well with the experimental data, especially at higher ionic strength values.

With the equations provided here and some elemental knowledge of computing software, the fast and accurate computation of equilibrium concentrations becomes feasible with the inclusion of the effects of ionic strength. In particular, we can now study multi-equilibria solutions with wide ranges of composition and ionic strength to improve on the parameters of the Debye–Hückel approximations and/or to explore conceptually improved theories of electrolyte solution.

5 Supplementary Material

9 pages are available: extended version of Table 1, two figures showing computed pH_{con} values of acetate-buffered acetic acid and of hydroxide titration of 0.2 $mol \cdot L^{-1}$ citric acid, and a figure showing species concentrations in the hydroxide titration of 0.2 $mol \cdot L^{-1}$ citric acid. Three figures for the hydroxide titration of 0.2 $mol \cdot L^{-1}$ triprotic model acid with pK_a values of 3, 6, and 9 show pH values as a function of added hydroxide, concentration quotients $\{-\log_{10}(Q)\}$ as a function of ionic strength (I), and concentrations of H_3A, H_2A^-, HA^{2-} and A^{3-} as a function of pH.

Acknowledgements Acknowledgement is made to the donors of the American Chemical Society Petroleum Research Fund for partial support of this research PRF-53415-ND4. This research was supported by NSF-PRISM grant Mathematics and Life Sciences (MLS, #0928053). M.A.D. has been supported as an MLS Fellow. EZ was supported by the Honors College Discovery Fellowship and the Arts & Sciences Undergraduate Research Mentorship Program.

References

1. Alberty, R.A.: Changes in the standard transformed thermodynamic properties of enzyme-catalyzed reactions with ionic strength. J. Phys. Chem. B **111**, 3847–3852 (2007)
2. Alberty, R.A.: Calculation of equilibrium compositions of systems of enzyme-catalyzed reactions. J. Phys. Chem. B **110**, 24775–24779 (2006)
3. Zidar, J., Merzel, F.: Probing amyloid-beta fibril stability by increasing ionic strengths. J. Phys. Chem. B **115**, 2075–2081 (2011)
4. Markarian, M.Z., Schlenoff, J.B.: Effect of molecular crowding and ionic strength on the isothermal hybridization of oligonucleotides. J. Phys. Chem. B **114**, 10620–10627 (2010)
5. Tong, W., Song, H., Gao, C., Möhwald, H.: Equilibrium distribution of permeants in polyelectrolyte microcapsules filled with negatively charged polyelectrolyte: the influence of ionic strength and solvent polarity. J. Phys. Chem. B **110**, 12905–12909 (2006)
6. Bolel, P., Datta, S., Mahapatra, N., Halder, M.: Exploration of pH-dependent behavior of the anion receptor pocket of subdomain IIA of HSA: determination of effective pocket charge using the Debye − Hückel limiting law. J. Phys. Chem. B **118**, 26–36 (2014)
7. Harris, D.C.: Quantitative Chemical Analysis, 8th edn. W.H. Freeman and Company, New York (2010)
8. Fox, S.I.: Cell Respiration and Metabolism. In: Fox, S.I. (ed.) Human Physiology, 13th edn, pp. 111–112. McGraw-Hill, New York (2013)
9. Santo-Domingo, J., Demaurex, N.: The renaissance of mitochondrial pH. J. Gen. Physiol. **139**, 415–423 (2012)
10. Ballantyne, J.S., Moyes, C.D.: The role of divalent cations and ionic strength in the osmotic sensitivity of glutamate oxidation in oyster gill mitochondria. J. Exp. Biol. **130**, 203–217 (1987)
11. Arena, G., Calì, R., Grasso, M., Musumeci, S., Sammartano, S.: The formation of proton and alkali-metal complexes with ligands of biological interest in aqueous solution. Part 1. Potentiometric and calorimetric investigation of H^+ and Na^+ complexes with citrate, tartrate, and malate. Thermochim. Acta **36**, 329–342 (1980)
12. McIlvaine, T.C.: A buffer system for colorimetric comparison. J. Biol. Chem. **49**, 183–186 (1921)
13. Voinescu, A.E., Bauduin, P., Pinna, M.C., Touraud, D., Ninham, B.W., Kunz, W.: Similarity of salt influences on the pH of buffers, polyelectrolytes, and proteins. J. Phys. Chem. B **110**, 8870–8876 (2006)
14. Salis, A., Bilaničová, D., Ninham, B.W., Monduzzi, M.: Hofmeister effects in enzymatic activity: weak and strong electrolyte influences on the activity of candida rugosa lipase. J. Phys. Chem. B **111**, 1149–1156 (2007)
15. Vandeventer, P.E., Lin, J.S., Zwang, T.J., Nadim, A., Johal, M.S., Niemz, A.: Multiphasic DNA adsorption to silica surfaces under varying buffer, pH, and ionic strength Conditions. J. Phys. Chem. B **116**, 5661–5670 (2012)
16. Akelis, L., Rousseau, J., Juskenas, R., Dodonova, J., Rousseau, C., Menuel, S., Prevost, D., Tumkevičius, S., Monflier, E., Hapiot, F.: Greener Paal-Knorr pyrrole synthesis by mechanical activation. Eur. J. Org. Chem. **1**, 31–35 (2016)

17. Pechini, M.P.: Method of preparing lead and alkaline earth titanates and niobates and coating method using the same to form a capacitor. US Patent 3,330,697 (1967)
18. Graca, M.P.F., Prezas, P.R., Costa, M.M., Valente, M.A.: Structural and dielectric characterization of $LiNbO_3$ nano-size powders obtained by Pechini. J. Sol–Gel. Sci. Technol. **64**, 78–85 (2012)
19. Wang, L.H., Yuan, D.R., Duan, X.L., Wang, X.Q., Yu, F.P.: Synthesis and characterization of fine lithium niobate powders by sol-gel method. Cryst. Res. Technol. **42**, 321–324 (2007)
20. Xia, H., Xiahou, Y., Zhang, P., Ding, W., Wang, D.: Revitalizing the Frens method to synthesize uniform, quasispherical gold nanoparticles with deliberately regulated sizes from 2 to 330 nm. Langmuir **32**, 5870–5880 (2016)
21. Aumiller, W.M., Bradley, W., Davis, B.W., Hashemian, N., Maranas, C., Armaou, A., Keating, C.D.: Coupled enzyme reactions performed in heterogeneous reaction media: experiments and modeling for glucose oxidase and horseradish peroxidase in a PEG/citrate aqueous two-phase system. J. Phys. Chem. B **118**, 2506–2517 (2014)
22. Garg, N.K., Mangal, S., Sahu, T., Mehta, A., Vyas, S., Tyagi, R.: Evaluation of anti-apoptotic activity of different dietary antioxidants in renal cell carcinoma against hydrogen peroxide. Asian Pac. J. Trop. Biomed. **1**, 57–63 (2011)
23. Choi, E.-Y., Kim, H.-J., Hana, J.-S.: Anti-inflammatory effects of calcium citrate in RAW 264.7 cells via suppression of NF-B activation. Environ. Toxicol. Pharmacol. **39**, 27–34 (2015)
24. Wang, F., Huang, P.-J., Liu, J.: Citrate inhibition of cisplatin reaction with DNA studied using fluorescently labeled oligonucleotides: implication for selectivity towards guanine. Chem. Commun. **49**, 9482–9484 (2013)
25. Glaser, R.E., Delarosa, M.A., Salau, A.O., Chicone, C.: Dynamical approach to multi-equilibria problems for mixtures of acids and their conjugated bases. J. Chem. Educ. **91**, 1009–1016 (2014)
26. Hoops, S., Sahle, S., Gauges, R., Lee, C., Pahle, J., Simus, N., Singhal, M., Xu, L., Mendes, P., Kummer, U.: COPASI: a complex pathway simulator. Bioinformatics **22**, 3067–3074 (2006)
27. Horn, F., Jackson, R.: General mass action kinetics. Arch. Ration. Mech. Anal. **47**, 81–116 (1972)
28. Dickenstein, A., Millán, M.P.: How far is complex balancing from detailed balancing? Bull. Math. Biol. **73**, 811–828 (2011)
29. Wu, J., Vidakovic, B., Voit, E.O.: Constructing stochastic models from deterministic process equations by propensity adjustment. BMC Syst. Biol. **5**, 187–208 (2011)
30. Strogatz, S.H.: Nonlinear Dynamics and Chaos: With Applications to Physics, Biology, Chemistry, and Engineering Studies in Nonlinearity. Westview Press, Boulder (2001)
31. Fuchs, A.: Nonlinear Dynamics in Complex Systems: Theory and Applications for the Life- Neuro- and Natural Sciences. Springer, New York (2013)
32. Verhulst, F.: Nonlinear Differential Equations and Dynamical Systems (Universitext). Springer, New York (2013)
33. Epstein, I.R., Pojman, J.A. (eds.): An Introduction to Nonlinear Chemical Dynamics: Oscillations, Waves, Patterns, and Chaos. Oxford University Press, New York (1998)
34. Gray, P., Scott, S.K.: Chemical Oscillations and Instabilities: Non-linear Chemical Kinetics. Oxford University Press, New York (1994)
35. Field, R.J., Gyorgyi, L. (eds.): Chaos in Chemistry and Biochemistry. World Scientific Publishing Co., Hackensack (1993)
36. Perrin, D.D., Dempsey, B.: Buffers for pH and Metal Ion Control. Chapman and Hall, London (1974)
37. Baeza-Baeza, J.J., García-Álvarez-Coque, M.C.: Systematic approach for the concentrations of chemical species in multiequilibrium problems: inclusion of the ionic strength effects. J. Chem. Educ. **89**, 900–904 (2012)
38. de Vicente, M.S.: Ionic strength effects on acid-base equilibria. Rev. Curr. Top. Solut. Chem. **2**, 157–181 (1997)
39. Brezonik, P.L.: Chemical Kinetics and Process Dynamics in Aquatic Systems, 1st edn. CRC Press, 155ff, Boca Raton (1993)
40. Butler, J.N.: Ionic Equilibrium: Solubility and pH Calculations. Wiley-Interscience, 41ff, New York (1998)
41. Partanen, J.I.: Prediction of activity coefficients of univalent electrolytes in pure aqueous solutions at 298.15 K by means of equations containing no adjustable parameters. Trends Phys. Chem. **11**, 31–60 (2006)
42. Davies, C.W.: Ion association and the viscosity of dilute electrolyte solutions. Part 1. Aqueous inorganic salt solutions. Trans. Faraday Soc. **60**, 2075–2084 (1964)
43. Burden, R.L., Faires, J.D.: Numerical Analysis. Cengage Learning, Boston (2010)
44. Wolfram Mathematica 9.0, Wolfram Research Inc.

45. Smith, W.R., Missen, R.W.: Using Mathematica and Maple to obtain chemical equations. J. Chem. Educ. **74**, 1369–1371 (1997)
46. Wolfram Mathematica 9.0 Documentation Center, Wolfram Research Inc. http://reference.wolfram.com/mathematica/ref/NDSolve.html (2016). Accessed 10 Dec 2016
47. Davies, C.W.: The extent of dissociation of salts in water. Part VIII. An equation for the mean ionic activity coefficient of an electrolyte in water, and a revision of the dissociation constants of some sulphates. J. Chem. Soc. (1938). doi:10.1039/JR9380002093
48. Bretti, C., De Stefano, C., Foti, C., Sammartano, S.: Critical evaluation of protonation constants. Literature analysis and experimental potentiometric and calorimetric data for the thermodynamics of phthalate protonation in different ionic media. J. Solution Chem. **35**, 1227–1244 (2006)
49. Long, F.A., McDevit, W.F.: Activity coefficients of nonelectrolyte solutes in aqueous salt solutions. Chem. Rev. **51**, 119–169 (1952)